

Composite Time-Frequency Analysis and Siamese Neural Network based Compound Interference Identification for Hopping Frequency System

Weiheng Jiang, Wanxin Yu, Jiangtian Nie, Zehui Xiong, Xiaogang Wu

Abstract—In a hostile environment, interference identification plays an important role in protecting the authorized communication system and avoiding its performance degradation. In this paper, the interference identification problem for the frequency hopping communication system is discussed. Considering presence of multiple and compound interference in the frequency hopping system, in order to fully extracted effective features of the interferences from the received signals, a composite time-frequency analysis method based on both the linear and bilinear transform is proposed. The time-frequency spectrograms obtained from the time-frequency analysis are constructed as matching pairs and input into the deep neural network for identification. In particular, the Siamese neural network is adopted as the classifier to perform the interference identification. That is, the paired spectrograms are input into the two sub-networks of the Siamese neural network to extract the features of the paired spectrograms. The Siamese neural network is trained and tested by calculating the gap between the generated features, and the interference type identification is realized by the trained Siamese neural network. The simulation results confirm that the proposed algorithm can obtain higher identification accuracy than both traditional single time-frequency representation based approach and the AlexNet transfer learning or convolutional neural network based methods.

Index Terms—Interference Identification, Time-frequency Analysis, Siamese Neural Network, Transfer Learning

I. INTRODUCTION

Anti-jamming plays an important role in guaranteeing the effective of wireless based command, control and communication system, especially in the hostile or adversarial environment [1], and interference identification is the prerequisite for realizing the anti-jamming. That is, only by knowing the type of interference that the wireless system is suffering, then it is possible to develop effective method for interference suppression or elimination. Till now, though lots of work have been done for the interference identification problem and many algorithms have been proposed for various wireless systems [2]–[20]. However, currently, the emergence of many new interference waveforms seriously degrade the performance of these algorithms [15]–[20]. In addition, due to the extreme nature of the electromagnetic environment and the intensity

of the confrontations, the amount of interference signal data that can be collected is limited. At the same time, with the development of deep learning theory these years [21], the capability of extracting effective features from limited samples is enhanced, thereby could be used to improve the accuracy of interference identification. Therefore, with deep learning, how to design interference identification algorithm with higher accuracy is an important research topic, especially for the case with limited samples and complicated interference environment, and it is the focus of this article.

Generally speaking, from the perspective of the application field, the research on interference identification mainly focuses on the radar system [2] and the wireless based communication system [3]–[20]. Since our focus is the later, thus the research status of this filed is summarized in the following.

By considering many systems are coexisting over the ISM band, interference identification and avoiding is an important issue for these systems and thus have been well discussed yet. Specifically, in [3], the WLAN interference identification under factory environments is discussed, scalogram time frequency images are computed from the collected received signal strength (RSS) data and then a convolutional neural network (CNN) is trained to recognize the spectral features and enable the interference classification. In [4], the authors present a semi-supervised deep learning (DL) based wireless interference identification (WII) algorithm which combines temporal ensembling technique with CNN network to exploit unlabeled data to improve the performance. In [5], a deep neural network based interference-classification method is proposed, in which both the power-spectral density (PSD) and the cyclic spectrum of the received signal as input features to the network. The computer experiments reveal that using the received signal PSD outperforms using its cyclic spectrum in terms of accuracy. Motivated by the increasing need for on-device interference detection and identification (IDI) for wireless coexistence, [6] develops a lightweight and efficient method targeting interference identification already at the level of single interference bursts. This method exploits real-time extraction of envelope and model-aided spectral features, specifically designed considering the physical properties of the signals captured with commercial off-the-shelf (COTS) hardware. [7] studies the problem of interference source identification, through the lens of recognizing one of 15 different channels that belong to 3 different wireless technologies, i.e., Bluetooth, Zigbee, and WiFi. Four different deep neural network architectures, i.e., CNN, ResNet, CLDNN, and

W. Jiang, W. Yu and X. Wu are with the Communication Measurement and Control Center, Chongqing University, Chongqing, China.(email: whjiang@cqu.edu.cn, wxyuwan@cqu.edu.cn, 1490626960@qq.com). J. Nie is with School of Computer Science and Engineering, Nanyang Technological University, Singapore.(email:jnie001@e.ntu.edu.sg). Z. Xiong is with Pillar of Information Systems Technology and Design, Singapore University of Technology and Design, Singapore.(email:zehui_xiong@sutd.edu.sg).

Manuscript received XXX, XX, 2015; revised XXX, XX, 2015.

LSTM are used as the classifier, the research demonstrated the generality of the effectiveness of deep learning at the considered task. In [8], a real-time external interference source classification method for an 802.15.4-based wireless sensor network using convolutional neural network is proposed. It uses RSSI sampling for collecting training and test data in an office environment. The output interference source type includes Wi-Fi beacon, different classes of WLAN traffic, BLE iBeacon, and microwave oven. The implementation on both IEEE 802.15.4 SoC and Linux-based system, experimental results showed that the proposed framework can classify the major interference types with high accuracy. Similarly, the authors of [9], [10] propose a wireless interference identification (WII) approach based upon a deep convolutional neural network (CNN) which classifies multiple IEEE 802.15.1, IEEE 802.11 b/g and IEEE 802.15.4 interfering signals in the presence of a utilized signal. The approach obtained a classification accuracy of approximately 100 % for IEEE 802.15.1 and IEEE 802.15.4 signals. For IEEE 802.11 b/g signals the accuracy increases for cross-technology interference with at least 90%. In [11], an unsupervised learning method and the unknown interference classifier are proposed based on the self-organizing map (SOM) neural network, the simulation results demonstrate that, the SNR reaches 5 dB, the accuracy of unknown interference classification exceeds 94%. More studies about the interference identification problem for WLAN and cellular system can be found in [12]–[14] for the interference identification in the WiFi system, inter-femtocell network and the C-RAN networks, respectively.

Besides the studies for traditional commercial networks, the interference identification for private or special communication networks also has drawn wide attentions, especially for the applications in the hostile or adversarial environment, such as for the frequency hopping or the direct sequence spreading spectrum (DSSS) based system. That is, in [15], for the time-slotted channel hopping (TSCH)-based industrial wireless sensor and actuator networks (IWSANs), a centralized interference classifier based on support vector machines (SVMs) is introduced. In [16], an iterative anti-interference method based on interference power cognition is proposed, where the interference is broadband digital modulation signal and desired signal is direct sequence spread spectrum (SS) signal. In [17], a blind user identification detection (UID) and interference identification scheme based on linear prediction algorithm for asynchronous direct-sequence code-division multiple-access systems over multipath fading channels is solved. Similarly, the work in [18] extracts 3dB bandwidth, time domain peak-to-average ratio and other features from the time-frequency domain information of the interference signal, and used decision tree and deep network classifiers to complete the classification of the interference signal. The authors in [19] proposes an interference recognition scheme based on a self-organizing map neural network, which improves the classification accuracy of known interference by 3.44%, and can reach an accuracy of 94% when the interference is unknown and the SNR is 5dB. The aforementioned methods mainly calculate traditional statistical features as classification features, while [20] mainly considers using linear time-frequency analysis to extract time-

frequency features containing mixed interference signals, and uses transfer learning to design classifiers. Compared with the traditional method, this method has higher accuracy, but there is a problem of lower time-frequency resolution during signal interleaving, and the demand for training samples is higher.

Based on the research status survey, we note that there are still many shortcomings for existing studies, especially for the hopping frequency wireless communication, which motivates the work of this paper. On the one hand, in practice and for the frequency hopping system, there may be multiple and compound interferences presented in the system, however, the already proposed algorithms only calculate traditional higher-order statistics or single time-frequency characteristics, thus their performance are limited for cannot effectively extract the signal features. On the other hand, mostly, all the existing studies used the support vector machine (SVM) or conventional neural network (CNN) as the classifier, training of these classifiers may require lots of samples and the obtained classification accuracy is low. Therefore, in order to improve the identification performance over complexity environment, especially for the hopping frequency system with multiple or composite interferences, we need to explore more effective methods for feature extracting and identification. Following that, in this paper, the interference identification problem for the frequency hopping communication systems is discussed and then a composite time-frequency analysis and Siamese neural network based interference identification algorithm is proposed. Specifically, the contributions of this paper are summarized as follows.

- Considering the presence of multiple and compound interference in the frequency hopping system, in order to fully extracted effective features of the interferences from the received signals to perform high precision interference identification, a composite time-frequency analysis method based on both the linear transformation and bilinear transformation is proposed.
- In addition, in order to realize high-precision interference identification with small samples, the Siamese neural network is adopted as the classifier. That is, the paired spectrograms are input into two sub-networks of the Siamese neural network, these two sub-networks extract the features of the paired spectrograms. Then the Siamese neural network is trained and tested for interference type identification by calculating the gap between the generated features.
- At last, the performance of the proposed algorithm is evaluated and analyzed by simulations. From the simulation results, we note that the identification accuracy of the proposed algorithm based on composite time-frequency analysis is better than the method based on single time-frequency transform in most cases. By performance comparison, we also noted that the proposed algorithm obtains higher identification accuracy than both the AlexNet transfer learning and the convolutional neural network based methods.

The rest of this paper is organized as follows. We briefly introduce the process of the proposed interference identification

algorithm in Section II. The details of the preprocessing steps for the interference identification algorithm, i.e., the composite time-frequency analysis, normalization, binarization, cropping and resizing are presented in Section III. We illustrate the architecture of the used Siamese neural network and its pre-training process in Section IV. The performance of the proposed algorithm is evaluated and analyzed in Section V and we conclude at last.

II. FLOW CHART OF INTERFERENCE IDENTIFICATION

A typical frequency hopping communication system includes a frequency hopping transmitter, wireless channel and a frequency hopping receiver. In which, the frequency hopping transmitter radiates the signal through the antenna after preprocessing and frequency hopping modulation. When the frequency hopping signal passes through the wireless channel, it will be affected by noise and interference. Therefore, the signal received by frequency hopping receiver is composed of frequency hopping modulated signal, interference and noise as

$$r(t) = s_1(t) + \sum_{i=2}^M s_i(t) + \sum_{j=1}^N J_j(t) + n(t). \quad (1)$$

Herein, $s_1(t)$ is the desired frequency hopping signal, $s_i(t), i = 1, \dots, M$ are the frequency hopping signals for other authorized receivers, i.e., they are the frequency hopping interference signals. $J_j(t), j = 1, \dots, N$ denote the potential jamming or interference signals which including fixed interference, periodic pulse interference, comb spectrum interference, periodic sweep interference and the mixed interferences. Specifically, the forms of these interference signals are given in the Appendix. $n(t)$ denotes the noise. In this paper, since the channel fading has a similar effect on the frequency hopping signals and the interference signals, thus to simplify the description, we ignore the channel effect hereafter.

In general, with the receiving signal (1), the frequency hopping receiver directly performs decoding after demodulating. However, if interference presents in the system, the receiver will face severe interference and direct signal demodulation will experience worse decoding performance [18]. Therefore, in order to protect the system and avoid performance degradation caused by potential interference, we need to perform interference identification and then interference suppression. While interference identification clarify the type of interference and obtain the parameters of the interference signals. As mentioned earlier, in this paper, we focus on identifying the type of interference signals presented in the system. And the proposed identification process is shown in Fig. 1. That is, at first, we implement a composite time-frequency analysis to obtain the spectrograms of the received signals. Based on that, we then construct the matching pairs of the obtained spectrograms, and the paired spectrograms are input into two sub-networks of the Siamese neural network. These two sub-networks extract the features of the paired spectrograms. Finally, the Siamese neural network is trained and tested for interference identification by calculating the gap between the generated features. In the sequel, the details of the composite

time-frequency analysis and Siamese neural network based interference identification method are presented.

III. COMPOSITE TIME-FREQUENCY ANALYSIS

As mentioned earlier, in order to implement interference identification, we should extract effective features from the interference signal. However, as we know that, if the interference signals are compounded with different types and also they are coincided with the frequency hopping signal, interference identification based on signal statistical characteristics such as instantaneous or high-order statistics will be greatly affected. This comes from the fact that, with compound interference signals, various time-domain, frequency-domain and instantaneous features of these interference signals and also the frequency hopping signals are affected or even canceled by each other. Thus it is difficult to effectively extract the typical time or frequency-domain features for these signals. To handle this issue, we propose a multi-channel composite time-frequency based method to achieve the feature extraction for the compound interference signals to assist interference identification. The core idea is that, both linear and bilinear time-frequency analysis methods are used to calculate the spectrograms of the received signals, and these spectrograms are used as features for identification. This is similar to the colored image recognition with ‘RGB’ multiple channels, three carefully chosen time-frequency analysis methods are adopted to formulate the ‘RGB’ channels for the interference identification, which takes the advantages of the complementarity of the capabilities of different time-frequency analysis tools. In this section, the details of the proposed multi-channel composite time-frequency method are presented.

A. Linear and Bilinear Time-Frequency Transforms

In this paper, both the linear and bilinear transform time-frequency methods are used to extract the features of the received signals. For the linear time-frequency transform, though there is no cross term, due to the existence of window functions, the resolution of time-frequency transform will be limited. Taking the short-time Fourier transform (STFT) as an example, the window function of STFT will affect both time resolution and frequency resolution, therefore, it is difficult to choose an optimal window function and set the appropriate parameters. Compared with STFT, wavelet transform can more effectively focus the instantaneous structure of the signal [22]. In addition, compared with the linear time-frequency transform, though the Cohen-like bilinear time-frequency transform introduces the cross terms, different time-frequency analysis effects can be obtained with different kernel functions. Therefore, in order to sufficiently extract enough time-frequency features, both the linear and the Cohen-like bilinear time-frequency transforms are adopted, i.e., we choose wavelet transform, MHD and BJD bilinear time-frequency transforms to obtain the spectrograms of the composite interference signals as follows, separately.

1) *Wavelet Transform*: Wavelets are wave-like transients that can be interpreted as sinusoids for short duration. Decomposition of a signal on the basis functions are called wavelet

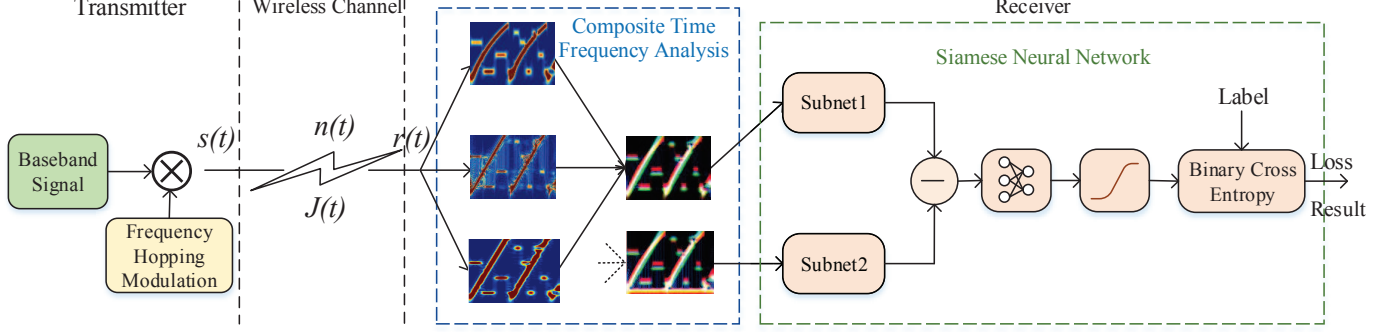


Fig. 1 Flow chart of interference Identification.

transforms (WTs). For the WTs, the width of the wavelet basis changes with frequency, i.e., if the frequency of the basis becomes larger, the time window width will automatically be narrowed to improve the resolution. Its principle is similar to a zoom camera [23]. Define the wavelet transform of a signal $s(t)$ as [24]

$$CWT_s(a, b) = \frac{1}{\sqrt{a}} \int_{-\infty}^{+\infty} s(t) \varphi\left(\frac{t-b}{a}\right) dt. \quad (2)$$

Herein, a and b are the scale (dilation) and translation parameters, respectively. The function $\varphi(t)$ is the basis function called the mother wavelet, and it is similar to the window function of the STFT. $\varphi(\frac{t-b}{a})$ is obtained by $\varphi(t)$ after translation and expansion transformation, and the basis function $\varphi(t)$ satisfies the following condition.

$$\int_{-\infty}^{+\infty} |\varphi(t)|^2 dt < \infty. \quad (3)$$

In this paper, the commonly Morlet wavelet basis function is used and who has the form

$$\varphi(t) = \frac{1}{\sqrt[4]{\pi}} e^{jw_0 t - \frac{t^2}{2}}. \quad (4)$$

2) *Margenau-Hill Distribution (MHD) Bilinear Transform*: It is a time-frequency analysis method with many excellent characteristics. Specifically, MHD has true marginality, weak supporting and better time-frequency aggregation [25]. MHD based bilinear transform can be characterized as

$$MHD_s(t, f) = \iint_{-\infty}^{+\infty} s(t + \tau/2) s^*(t - \tau/2) \cos(\eta\tau/2) \cdot e^{-j2\pi(\eta t + f\tau - \eta u)} d\tau. \quad (5)$$

From the above, we can note that the kernel function of MHD is $\phi(\eta, \tau) = \cos(\eta\tau/2)$ and it is more complexity than that for Wigner-Ville distribution (WVD). Similar to pseudo-Wigner-Ville distribution (PWVD), if the time domain window function $h(\tau)$ is added to the time domain variable τ , the cross term of MHD can be suppressed to a certain extent and which forms a pseudo Margenau-Hill distribution (PMHD).

3) *Born-Jordan distribution (BJD) Bilinear Transform*: The kernel function of BJD is $\phi(\eta, \tau) = \sin(\pi\tau\eta)/\pi\tau\eta$. Compared with other Cohen-like time-frequency analysis methods, BJD has higher time-frequency resolution. And its expression is

$$BJD_s(t, f) = \frac{1}{2a} \int_{-\infty}^{+\infty} \frac{1}{|\tau|} \int_{t-a|\tau|}^{t+a|\tau|} s(u + \tau/2) s^*(u - \tau/2) \cdot e^{-j2\pi f\tau} du d\tau, \quad (6)$$

where a is constant.

Therefore, for the received signals, above linear and bilinear time-frequency analysis methods, i.e., the wavelet transform, MHD transform and BJD transform, are used to calculate the spectrograms to formulate the inputs for the three channels of the deep networks, as shown in Fig. 2. That is, the grayscale images obtained from these three time-frequency transforms are used as the red, green and blue (RGB) sub-images, respectively. Subsequently, during the deep network training, these sub-images are input into the neural network as three channels of the deep network. Herein, the three channels of the composite spectrograms retain the characteristics of three time-frequency analysis methods, including both linear and nonlinear time-frequency analysis characteristics. However, in order to better extract the features and perform training and classification by the deep network, some preprocessing steps are required, i.e., the image normalized, binarized, cropped and resized, which will be explained as below.

B. Image Normalization

Due to the fact that, by performing time-frequency transform, the pixel value of the gray-scale spectrogram $I(x, y)$ for different kinds of interference signals may significantly different, and the data (image) with larger pixel value will have a greater impact on training, thereby destroying the balance of the data set. In order to reduce the imbalance of the data set, the gray-scale spectrogram is normalized before inputting into the deep network. That is, for the gray-scale spectrogram $I_1(x, y)$, the normalization method is

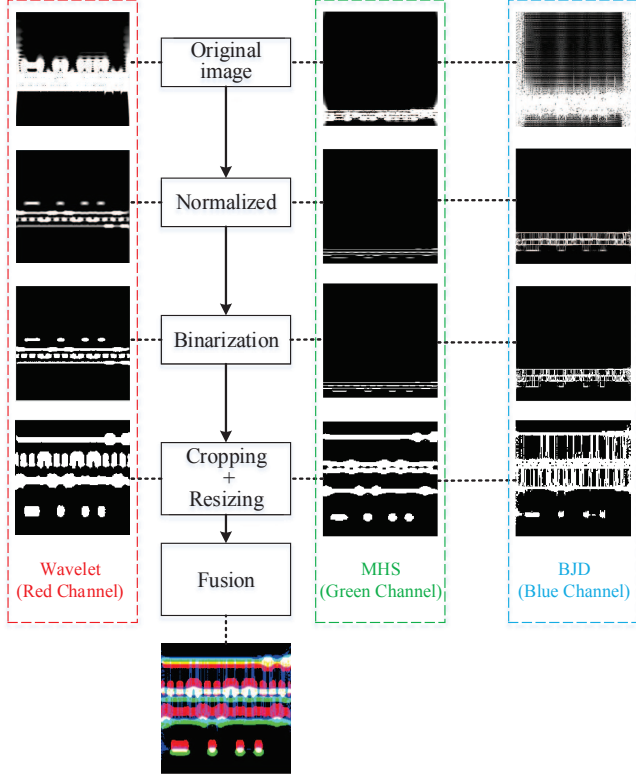


Fig. 2 Flow chart of composite time-frequency analysis.

$$I_1(x, y) = \begin{cases} 0, & I(x, y) \leq a_{\min} \\ \frac{I(x, y) - a_{\min}}{a_{\max} - a_{\min}}, & a_{\min} < I(x, y) < a_{\max} \\ 1, & I(x, y) \geq a_{\max}, \end{cases} \quad (7)$$

where a_{\min} and a_{\max} are the minimum and maximum thresholds. That is, the pixel value smaller than a_{\min} is set to 0, and the pixel value larger than a_{\max} is set to 1. In this article, a_{\min} and a_{\max} are set to 0 and 137, respectively.

C. Image Binarization

The binarization algorithm used in this paper is based on a global threshold [26]. In particular, the binarization algorithm is summarized as **Algorithm 1** shown below.

D. Image Cropping and Resizing

From Fig. 2, we note that most areas of the image after binarization contain no useful features. Therefore, in order to reduce redundant information of the image, part of the image has no useful information is cropped. That is, we carry out frequency domain clipping according to the start and end frequencies of the frequency hopping signal and also the highest and lowest frequencies of the interference signal, but does not cut in the time domain. In addition, in order to further reduce the amount of data and adapt to the input of the deep network, the size of the cropped image is adjusted so that all the images generated by the time-frequency transforms

Algorithm 1 Binarization algorithm

- 1: **Input:** Normalized time-frequency grayscale image $I_1(x, y)$;
- 2: **repeat**
- 3: **Initialize:** Threshold $T = (\max_{x,y}(I_1(x, y)) + \min_{x,y}(I_1(x, y)))/2$;
- 4: Use T to divide image $I_1(x, y)$ into two parts H_1 and H_2 , where H_1 includes pixels with a value greater than T , and H_2 includes other values;
- 5: Calculate the average values μ_1 and μ_2 of H_1 and H_2 , respectively;
- 6: Update $T = (\mu_1 + \mu_2)/2$;
- 7: **until** $\Delta T \leq 0.001$;
- 8: $I_B(x, y) = \begin{cases} 1, & I_1(x, y) \geq T, \\ 0, & \text{otherwise.} \end{cases}$;
- 9: **Output:** $I_B(x, y)$.

have the same size. Specifically, we use the nearest neighbor interpolation algorithm in image resizing as [27].

To sum up, for each sample signal (received by the frequency hopping receiver), at first, we perform the wavelet based linear time-frequency transform, MHD and BJD based bilinear time-frequency transforms to obtain three gray-scale spectrograms. Then aforementioned normalization, binarization, cropping and size adjustment are sequentially used for the three gray-scale spectrograms. In order to make full use of the characteristics of linear and Cohen-like bilinear time-frequency transforms, the three single-channel gray-scale time-frequency images are transferred to the red, green and blue colored images, respectively, to formulate the three-channels RGB color spectrograms and finally input into the deep neural network for identification.

IV. SIAMESE NEURAL NETWORK

The Siamese neural network was first introduced by Bromley and LeCun in the early 1990s to solve the problem of signature verification in the form of image matching [28]. The Siamese neural network is composed by two sub-networks that accept different inputs and a top energy function. The energy function at the top calculates the distance between the topmost output feature representations of the sub-networks on both sides. The parameters between the two sub-networks are bound, so that the two sub-networks calculate the characteristics of their respective input samples according to the same rules [29]. In the following, the architecture and the parameters of the Siamese neural network used in this paper are presented.

A. Architecture of the Siamese Neural Network

The architecture of the Siamese neural network is shown in Fig. 3. It contains L layers, and each layer of the sub-network contains N_l neurons, where $\mathbf{h}_{1,l}$ represents the hidden layer vector of the l th layer of sub-network 1, and $\mathbf{h}_{2,l}$ represents the hidden layer vector of the l th layer of sub-network 2. The rectified linear (ReLU) unit is used as the activation function in the first $L - 1$ layers of the Siamese neural

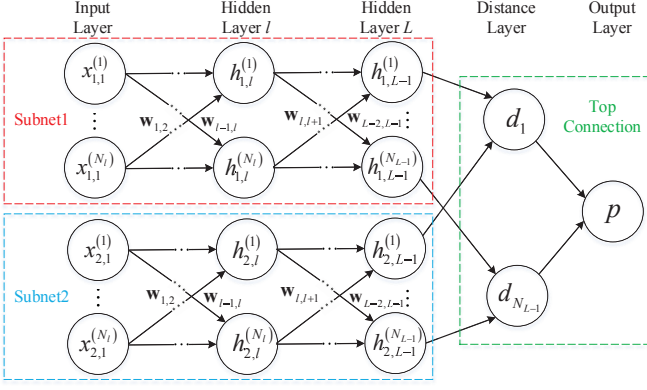


Fig. 3 Architecture of the Siamese neural network.

network. Therefore, $\forall l \in \{1, \dots, L-1\}$, we have the following relationship for the Siamese neural network,

$$h_{1,m} = \max(0, \mathbf{W}_{l-1,l}^T \mathbf{h}_{1,(l-1)} + \mathbf{b}_l), \quad (8)$$

$$h_{2,m} = \max(0, \mathbf{W}_{l-1,l}^T \mathbf{h}_{2,(l-1)} + \mathbf{b}_l). \quad (9)$$

Herein, $\mathbf{W}_{l-1,l}$ represents the shared weight matrix of the two sub-networks connecting the N_{l-1} neurons of the $(l-1)$ th layer and the N_l neurons of the l th layer, the size is $N_{l-1} \times N_l$, and \mathbf{b}_l is the bias vector of the l th layer.

After the $L-1$ layers feedforward network, we then use the distance layer to quantify the difference of the eigenvectors $\mathbf{h}_{1,L-1}$ and $\mathbf{h}_{2,L-1}$ calculated by the two sub-networks. The distance function used by the distance layer is

$$p = \sigma \left(\sum_j \alpha_j \left| \mathbf{h}_{1,l}^{(j)} - \mathbf{h}_{2,l}^{(j)} \right| \right), \quad (10)$$

herein, $\sigma(\cdot)$ is the sigmoidal activation function. This final distance layer induces a metric on the learned feature space of the $L-1$ th hidden layer, and scores the similarity between the two feature vectors, and finally obtains the predicted score p . α_j are additional parameters learned by the model during the training process, which weighting the importance of the component-wise distance. This defines a final L th fully-connected layer for the network which joints the two Siamese twins.

B. Parameters of the Siamese Neural Network

The sub-network architecture of the Siamese neural network used in this paper is shown in Fig. 4. The parameters of the two sub-networks are bounded and they have the same network architecture. That is, each sub-network is composed of 4 convolutional layers. Each convolutional layer uses a different size of convolution kernel, and the fixed step size is 1. The number of convolution kernels is designated as a multiple of 16, which can facilitate the training process and optimize the performance. The middle convolutional layer of the sub-network uses the ReLU function as the activation function to perform output feature mapping and then it is followed by a maximum pooling layer with a step size of 2. While

after the last convolutional layer is a fully connected layer, the sigmoidal activation function is used for mapping for the fully connected layer. The Adam optimizer is adopted for the sub-network training, and the learning rate is dynamically adjusted. By gradually reducing the learning rate, the network can more easily converge to a minimum.

V. SIMULATION RESULTS

In this section, the performance of the proposed compound time-frequency analysis and Siamese neural network based interference identification algorithm is evaluated and analyzed. Herein, we first introduce the training parameters for the Siamese neural network and the parameters used to generate the interference signal data set. Then we present some time-frequency analysis results of the interference signals under different scenarios and analyze how does the spectrograms are affected by the system parameters. Finally, the interference identification performance of the proposed algorithm is verified and analyzed by simulations.

A. Simulation Parameters and Data Set Construction

1) *Siamese Network Training Parameters*: The parameters used for training of Siamese neural network are listed in TABLE I. The parameters adopted by the two sub-networks are bounded and updated synchronously to perform fairly feature mapping for the input images. Herein, $N(\mu, \sigma^2)$ represents a normal distribution with mean value μ and variance σ^2 .

TABLE I Training parameters of the Siamese network

| Parameters | Value |
|------------------------------------|----------------|
| Weighting initialization value | $N(0, 0.01)$ |
| Bias initialization value | $N(0.5, 0.01)$ |
| Learning rate initialization value | $6e-5$ |

2) *Parameters for Signal Sample Generation*: The parameters used in the simulations for the frequency hopping communication system are shown in TABLE II, as [20], we consider a low-speed frequency hopping system.

TABLE II Parameters of frequency hopping signal

| Parameters | Value |
|-----------------------------|---------------------|
| Signal modulation method | 2PSK |
| Number of frequency hopping | 16 |
| Frequency set | [100,220]kHz |
| Rate | 100 hops per second |
| Sampling frequency | 16MHz |

While the parameters for the interference signals are set as TABLE III [20], in which $U[a, b]$ represents the uniform distribution on the interval $[a, b]$. That is, four kinds of interference are considered, i.e., fixed frequency interference, periodic linear sweep interference, periodic pulse interference and comb spectrum interference.

Also, in simulations, the interference signal strength is measured by the jamming-to-signal power ratio (JSR) defined as (11), where $V_{Jamming}$ and V_{Signal} denote the average amplitudes of the interference signal and the frequency hopping signal, respectively.

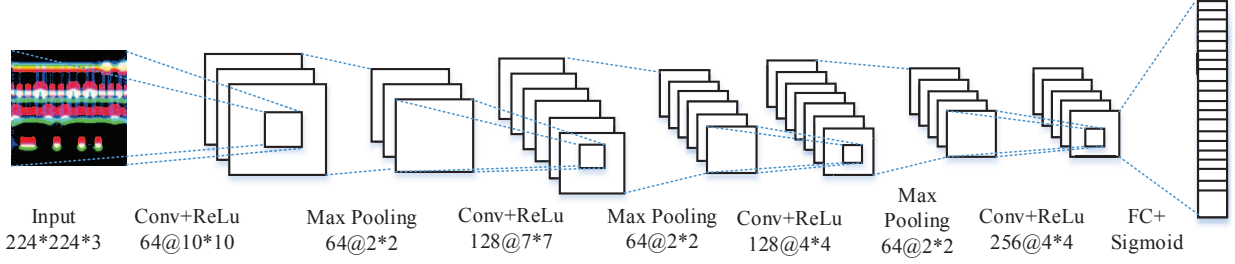


Fig. 4 Architecture of the sub-network of the Siamese neural network.

TABLE III Parameters of interference signal

| Type | Parameters | Value |
|------------------------------------|----------------------|-------------------|
| Fixed frequency interference | Frequency set | 80,160,200kHz |
| | Sweep bandwidth | $U[50, 100]$ kHz |
| Periodic linear sweep interference | Sweep period | $U[1e-6, 5e-6]$ s |
| | Start frequency | $U[0, 100]$ kHz |
| Periodic pulse interference | Pulse period | $U[3e-5, 8e-5]$ s |
| | Duty ratio | $[0.2, 0.5]$ |
| Comb spectrum interference | Number of comb teeth | $[4, 8]$ |
| | Comb frequency | $[90, 210]$ kHz |

$$JSR = -20 \lg \frac{V_{Jamming}}{V_{Signal}} \quad (11)$$

To generate signal sample and data set, the value of JSR varies from -10dB to 20dB with an interval of 5dB, i.e., we have 7 values of JSR. In addition, besides the singularity interference shown in TABLE III, we also consider the combination interference in the simulations. However, for the combination interference, we only discuss a combination of two kinds of interference. Therefore, there are $C_4^1 + C_4^2 = 10$ types of interference. Unless otherwise stated, the training data set is generated as follows, for each value of JSR and the type of interference, 100 signal samples are randomly generated, i.e., we totally have $7 \times 10 \times 100 = 7000$ signal samples. In addition, when generating the data set, the amplitudes of all interference signals are uniformly distributed over $[0.5, 1.5]$. It should be noted that, the data input to the Siamese network is in the paired form. In particular, we randomly select two samples in the training set as the matching pairs. If the two samples of the matching pair have the same type, the label of the matching pair is 1, otherwise the label of the matching pair is 0. Furthermore, the Siamese neural network is iteratively trained 2000 times, and 180 matching pairs are randomly generated from the training set for each iterative training, so a total of 360,000 training matching pairs are included.

B. Time-frequency Spectrogram for the Signals

In this subsection, the time-frequency spectrograms of the composite interference signals are analyzed. To facilitate the

analysis of the simulation results, herein, the number of hopping frequencies for the considered system is set to 4.

1) *The Time-Frequency Spectrogram for Different Time-frequency Methods:* First, taking the frequency hopping signal interfered by the periodic linear sweep interference signal as an example, we analyze the time-frequency features extracted by different time-frequency analysis methods, i.e., Wavelet, MHD and BJD, in which the JSR is set to 0dB. The results are shown in Fig. 5. While the horizontal axis of the time-frequency spectrogram is time and the vertical axis is frequency. The gradation of the color in the spectrogram indicates the normalized power intensity of the signal. It can be found from Fig. 5 that, for all the mentioned time-frequency analysis methods, the spectrograms of the frequency hopping signal exhibit the characteristics of time-varying and frequency hopping in the time-frequency domain, while the linear frequency sweeping signal shows the characteristic of linearly frequency changing with time in the time-frequency domain. Therefore, all the above-mentioned time-frequency analysis methods can extract the frequency hopping characteristics of the frequency hopping signal and the frequency gradual change characteristics of the periodic linear frequency sweep signal. Moreover, we can note that, the main difference among the spectrograms obtained by different time-frequency analysis methods is that when the signals overlap, the Cohen-like bilinear time-frequency representations, especially the BJD time-frequency transform using the kernel function $\phi(\eta, \tau) = \sin(\pi\tau\eta)/(\pi\tau\eta)$, has abundant cross terms. This is confirmed by the overlap part of the frequency hopping and frequency sweep signals in Fig. 5(c). Compared with the features shown in Fig. 5(a), BJD time-frequency analysis has more crossover features and fine image branches. In addition, for the proposed composite time-frequency analysis, the characteristics of linear and nonlinear time-frequency analysis are retained as that shown in Fig. 5(d), which can be used to enhance the identification performance.

2) *Time-frequency Spectrogram for Different Kinds of Interference:* Now, the time-frequency spectrogram of the signals interfered by one of the aforementioned four kinds of singularity interferences or two kinds of composite interferences are analyzed. Herein, the JSR of the signals are set to 0dB and the Wavelet transform is taken as an example. The results are shown in Fig. 6. In which, Fig. 6(a) is the case that the signal is interfered by fixed-frequency interference. And from the time-frequency spectrogram, we can observe single

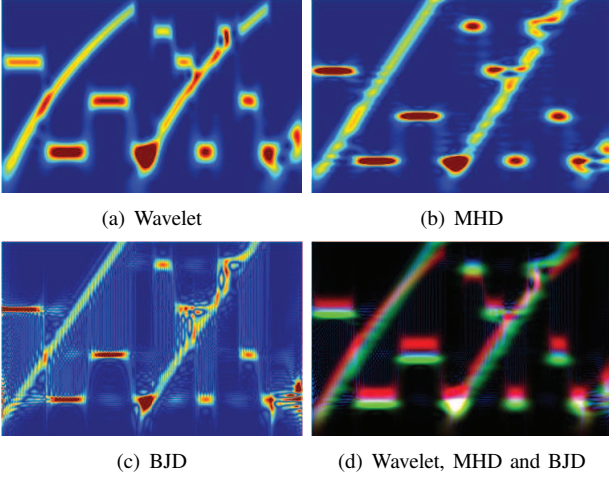


Fig. 5 Spectrogram images of interference signals with different TFD.

or multiple interference signals on one fixed frequency or multiple frequencies, they are corresponding to single-tone and multi-tone interferences, respectively. We note that this type of interference has a great impacts for the frequency hopping signal appearing in its frequency range. For periodic linear frequency sweep interference, as shown in 6(b), the interference signal is continuous in frequency domain and appears as a diagonal band in the spectrogram, which can interfere with a wide range of frequencies. The periodic pulse interference shown in Fig. 6(c) contains multiple frequency bands with gradual power intensity in the spectrogram. The pulse period affects the distance between frequency bands in the spectrogram, and the duty cycle affects the distribution of distance between frequency bands in the spectrogram. For comb spectrum interference, as shown in Fig. 6(d), in the interference frequency band, continuous interference frequency bands appear, corresponding to each comb tooth of comb spectrum interference.

In the case of multiple interferences coexisting, the time-frequency spectrogram will contain multiple interference characteristics. If the time-frequency characteristics of different types of interferences are significant different, it is still easy to perform interference identification, such as that shown in Fig. 6(e), where the interference is composite by fixed frequency and linear frequency sweep signals. The problem becomes challenge as the composite interferences have similar time-frequency characteristics, such as that shown in Fig. 6(f) where the interference is composite by periodic pulse and comb spectrum signals.

3) *The Influence of JSR*: At last, we analyze how does the time-frequency spectrogram is affected by interference signal intensity by varying the value of JSR and the result is shown in Fig.7. Herein, taking the frequency hopping system is interfered by the composite of sweeping and fixed frequency interferences as an example, and using Wavelet transform as the time-frequency analysis tool. It can be seen from the figure that with the increase of JSR, the color of the interference signal in the time-frequency spectrogram becomes darker and covers each other, especially as JSR=20dB, that

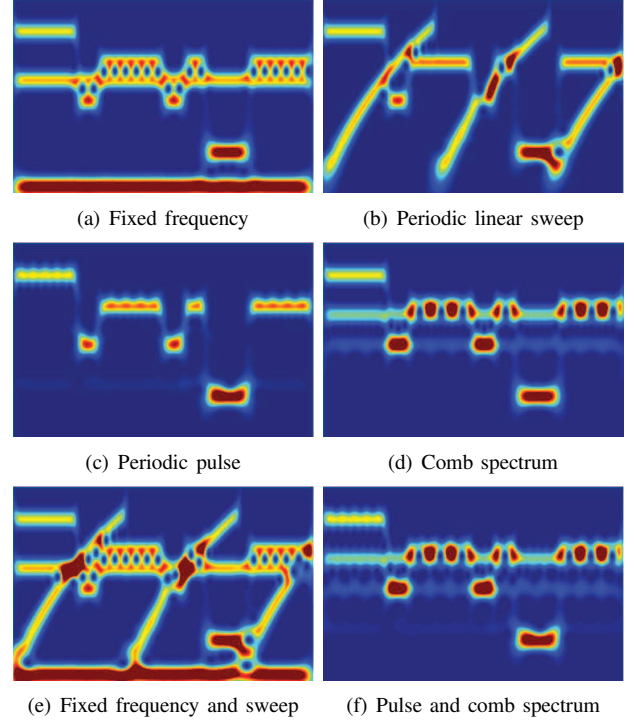


Fig. 6 Spectrogram images of different interference signals.

is, the interferences are strong enough so that the features of different kinds of interferences are overlapped, thus the interference signal aliasing in the spectrogram and seriously reducing the distinguishability of them. While as JSR=-10dB, the interference intensity is low, now the interference is not obvious in the spectrogram and thus it is more difficult to distinguish the interference signals with similar characteristics. In fact, if JSR is small, there is no need to perform interference identification as it may not interfere the authorized communication system.

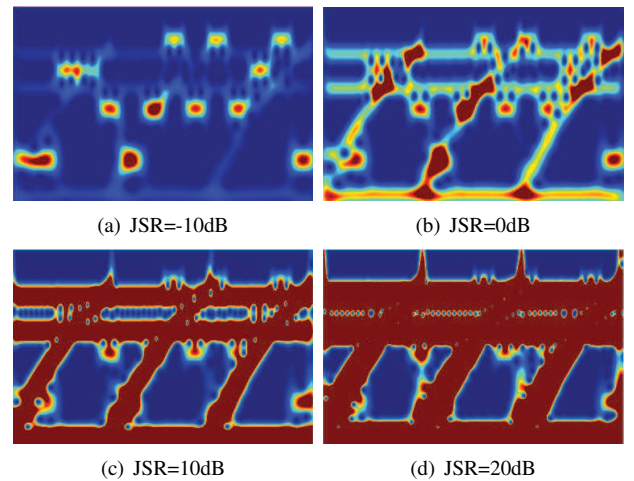


Fig. 7 Spectrogram images of interference signals at different JSRs.

C. Performance of the Algorithm

In this subsection, the performance of the proposed interference identification algorithm is evaluated. At first, we explore how does the algorithm performance is affected by different time-frequency transforms. We then evaluate and analyze the algorithm performance by comparing it with traditional convolutional neural network and AlexNet transfer learning based interference identification algorithms. Finally, we further discuss the impact of sample data set size on the performance of the interference identification algorithm.

1) *Analysis the effect of composite time-frequency analysis method:* In order to verify the effect of the composite time-frequency analysis method on improving the performance of the interference identification algorithm, we analyze the classification accuracy of the interference identification algorithm based on linear, Cohen bilinear and composite time-frequency analysis method. The parameters used for training of the Siamese network and also the data set generation are as described in Section V-A. Fig. 8 shows the trend of the loss objective function during the training process of the Siamese network. It can be seen from the figure that after batch training, the loss function value gradually stabilizes, and the Siamese network gradually converges.

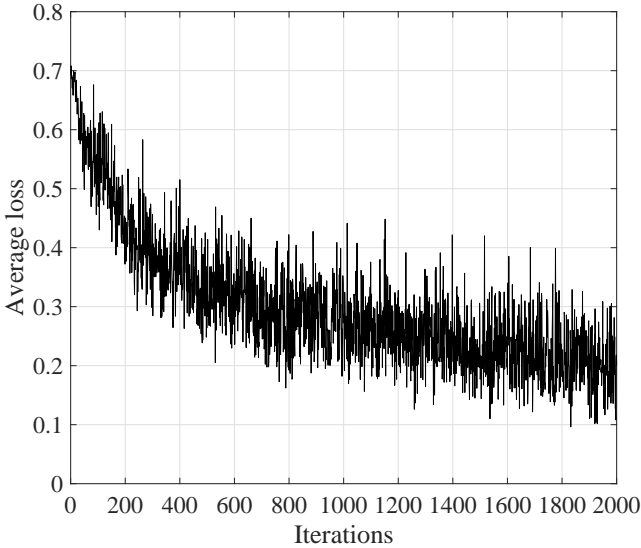


Fig. 8 The training loss of the Siamese network.

Fig. 9 shows how does the identification accuracy is affected by different time-frequency analysis methods, where the average classification accuracy is calculated herein and it is an average accuracy for identifying 10 kinds of interference. It can be seen from the figure that if JSR does not exceed 15dB, as JSR increases, the classification accuracy of different time-frequency analysis methods are all gradually improved, i.e., the intensity of interference increases and the features of the interference signals become obvious which facilitates the identification. While if JSR exceeds 15dB, the classification accuracy decreases. This phenomenon comes from the fact that, if JSR becomes larger, the interference signal intensity will be too larger so that a large area of the spectrogram is

covered by the high-power signal features and the pixels color of the spectrogram becomes darker, i.e., part of the unique features of interference signal will be concealed, especially when the interferences are overlapped. This has been verified by time-frequency spectrogram shown in Section V-II.

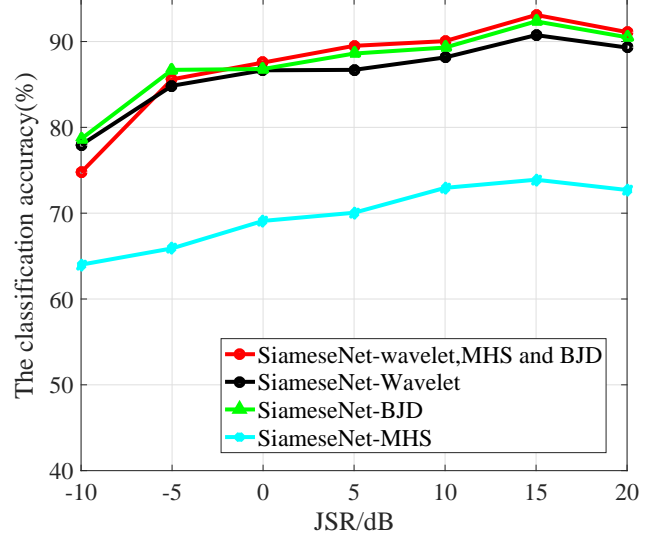


Fig. 9 Classification accuracy of different time-frequency analysis methods versus JSR.

From Fig. 9, we can observe that, MHD based method has the lowest classification accuracy, followed by wavelet based method, and BJD based method obtains the highest accuracy among the single time-frequency analysis based methods. Also we note that, when the interference signal intensity is large, i.e., $JSR \geq 0dB$, the composite time-frequency analysis based interference identification algorithm obtains the highest classification accuracy. While the situation becomes worse as $JSR < 0dB$, that is, as the interference signal intensity is too weak, the classification accuracy of the compound time-frequency analysis based method is slightly lower than the BJD time-frequency analysis based method. This result comes from the fact that, as the interference signal intensity is very low, the cross term generated by the BJD time-frequency transform can enhance the distinguishability of different kinds of interferences. However, though BJD, MHD and Wavelet transforms are combined in our composite time-frequency analysis method, the features obtained from this composite time-frequency analysis may be ignored thus achieve worse performance. In spite of this, this result still confirms that in most cases, the proposed composite time-frequency analysis based algorithm can obtain better performance than the other single time-frequency analysis based approaches.

2) *Analysis the effect of Siamese Network:* In order to fully characterize the performance of the proposed algorithm, we further analyze the effect of Siamese network and its performance by comparing it with the AlexNet transfer learning and the convolutional neural network based algorithms. The parameters of AlexNet can be found in [30]. The core idea of the AlexNet transfer learning based interference identification algorithm is that, use the pre-trained AlexNet network and

adaptive the last three layers of the network to our interference identification problem, and then the same data set is used to fine-tune the parameters of obtained AlexNet network. The configurations for the convolutional neural network are three convolutional layers with an *ReLU* active function for each convolutional layer, then followed by a maximum pooling layer, and the last layer of the whole network is a fully connected layer. In comparison, the same data set described in Section V-A is used by the three networks for testing and training.

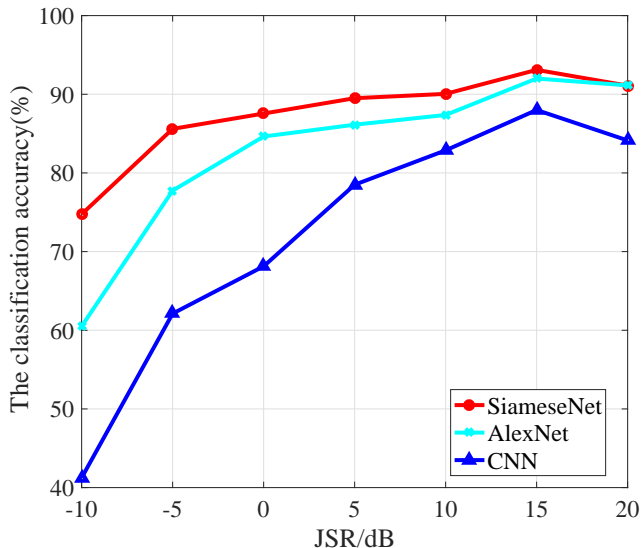


Fig. 10 Classification accuracy of different neural network versus JSR.

Fig. 10 shows the identification results of aforementioned three networks. Still, it can be seen from the figure that as JSR does not exceed 15dB, as JSR increases, the classification accuracy of all algorithms gradually increases. While as JSR exceeds 15dB, the classification accuracy of all three networks are reduced. This phenomenon is consistent with that shown in Fig. 9 and has the same reasons thus omitted for simplification. In addition, we also can note that the Siamese network based algorithm obtains the highest classification accuracy, followed by the AlexNet transfer learning based algorithm, and the convolutional neural network based algorithm has the lowest classification accuracy. This result verifies the dominated performance of the proposed Siamese network based algorithm over the AlexNet transfer learning and the convolutional neural network based algorithms.

3) *Analysis the impact of sample data set size*: In order to evaluate the performance of the algorithm on small data sets, we further verify the identification performance of the Siamese network with different training matching pairs. That is, under the condition that the total number of training samples is unchanged, TABLE IV shows how does the classification accuracy is varying with the training matching pairs of the Siamese network. The average classification accuracy in the table is an average interference classification accuracy under various JSR. One can note that, as the number of matching pairs decreases, the average classification accuracy decreases,

while as the number of iterations and the number of matching pairs in each batch of training decreases, the classification accuracy also decreases. However, the reduction in the number of matching pairs does not significantly reduce the classification accuracy. In addition, it is worth mentioning that the average classification accuracy of the aforementioned two comparison algorithms, namely, the AlexNet transfer learning and the convolutional neural network based algorithms are 82.79% and 72.14%, respectively. It can be seen that even if fewer matching pairs are used by the Siamese network during the training process, its interference classification accuracy is still higher than the AlexNet transfer learning and the convolutional neural network based algorithms. The main reason is that, in order to generate training matching pair samples, the random matching is used by the Siamese network, thus the trained Siamese network is more robust in interference classification than the AlexNet transfer learning and the convolutional neural network based algorithms. This result also confirms the dominated performance of the proposed Siamese network based algorithm.

TABLE IV Effects of the number of training sample and matching pair on Siamese network

| Training samples | Iterations | Matching pairs per iteration | Total matching pairs | Average recognition accuracy(%) |
|------------------|------------|------------------------------|----------------------|---------------------------------|
| 7000 | 2000 | 180 | 360000 | 87.38 |
| 7000 | 2000 | 100 | 200000 | 86.99 |
| 7000 | 1000 | 180 | 180000 | 86.34 |
| 7000 | 1000 | 100 | 100000 | 85.92 |

VI. CONCLUSION

In this paper, the interference identification problem for the frequency hopping communication systems is discussed and then a composite time-frequency analysis and Siamese neural network based interference identification algorithm is proposed. Specifically, in order to fully extract the characteristics of various interferences, at first, a composite time-frequency analysis algorithm is designed to calculate the time-frequency distribution of the interference signal. That is, both the linear time-frequency transform, i.e., Wavelet transform, and the bilinear time-frequency transform, i.e., MHD and BJD transforms, are used to extract the time-frequency representations of the interference signals, and thus three-channel time-frequency spectrograms are obtained. Then before the multi-channel time-frequency spectrograms are input to the deep network for identification, they are normalized, binarized, resized and cropped. Finally, the Siamese network is selected as the classifier. In which, the twin sub-network of the Siamese neural network calculates two distance vectors of the input samples on each sub-network to determine whether the two inputs are the same type of samples. The matching and identification of the samples are realized after repeated training. From the simulation results, we found that the identification accuracy of the proposed algorithm based on composite time-frequency analysis is better than the method based on single time-frequency transformation in most cases. In addition, through comparison, we also noted that the proposed algorithm obtains

higher identification accuracy than both the AlexNet transfer learning and the convolutional neural network based methods.

APPENDIX A TYPICAL INTERFERENCE PATTERNS

According to the interference pattern, there are four kinds of interferences for the wireless communication system, i.e., fixed interference, sweep interference, periodic pulse interference and comb spectrum interference. The forms of these interference signals are presented below.

Fixed interference: It performs continuous interference at a specific frequency, the interference signal form is

$$J(t) = \sum_{i=1}^N A_i \cos(2\pi f_i t + \phi_i). \quad (12)$$

Where N denotes the number of interference frequencies, if $N = 1$, it is degenerated to the monophonic interference, while if $N > 1$, it is termed as multi-tone interference. In addition, A_i , f_i and ϕ_i represent the amplitude, frequency and initial phase of the i th interference signal, respectively. The key parameters for the fixed frequency interference are f_i , N and A_i .

Sweep interference: It is a suppressive interference that scans each frequency in a designated frequency band to destroy all the authorized signals over this frequency band. In this paper, we only consider the periodic linear sweep interference and the signal form with single period is

$$J(t) = A \cos(2\pi f_0 t + \pi \mu_0 t^2 + \phi_0). \quad (13)$$

Where A , f_0 , μ_0 and ϕ_0 denote the amplitude, initial frequency, sweep slope and initial phase of the sweep interference, respectively. In practical, the sweep interference is periodically performed over a designated frequency band and the main parameters are the scanning cycle and sweep slope.

Periodic pulse interference: It is an interference signal composed of a narrow pulse sequence. The signal form is

$$J(t) = \sum_i A g_\tau(t - iT). \quad (14)$$

Where A and T denote the amplitude and pulse repetition period of the periodic pulse interference signal, respectively, and $g_\tau(\cdot)$ represents a rectangular pulse with pulse width τ . In addition, for the periodic pulse interference, there is an inexplicit parameter, i.e., the duty factor γ , and it is defined as $\gamma = \tau/T$. The key parameters for the periodic pulse interference signals are the pulse width τ , repetition period T and the duty factor γ .

Comb spectrum interference: It is a kind of discrete blocking interference and it has multiple discrete narrow band interferences over a designated frequency band. The signal form is

$$J(t) = \sum_{i=1}^N A_i(t) \cos(2\pi f_i t + \phi_i(t)). \quad (15)$$

Where N , $A_i(t)$, f_i and $\phi_i(t)$ represent the number of comb, envelope, comb frequency and phase of the comb frequency interference signals, respectively. We can note that, the comb frequency interference is a superposition of N narrow band

interference signals. For the comb interference signals, the bandwidth, envelope, the gap among the combs are all adjustable parameters.

REFERENCES

- [1] W. Zhang, *Handbook of cognitive radio*. Springer Singapore, 2017.
- [2] J. Kim, S. Lee, Y. Kim, and S. Kim, "Classification of Interference Signal for Automotive Radar Systems With Convolutional Neural Network," *IEEE Access*, vol. 8, pp. 176717–176727, 2020.
- [3] J. Webberet *et al.*, "WLAN Interference Identification Using a Convolutional Neural Network for Factory Environments," *J. Commun.*, vol. 8, no. 7, pp. 276–283, 2021.
- [4] J. Huang *et al.*, "Semi-supervised deep learning based wireless interference identification for iiot networks," in *VTC-Fall*, 2020, pp. 1–5.
- [5] J. Yu, M. Alhassoun, and R. M. Buehrer, "Interference classification using deep neural networks," in *VTC-Fall*, 2020, pp. 1–6.
- [6] S. Grimaldi, A. Mahmood, and M. Gidlund, "Real-time interference identification via supervised learning: Embedding coexistence awareness in iot devices," *IEEE Access*, vol. 7, pp. 835–850, 2019.
- [7] X. Zhang *et al.*, "Deep learning for interference identification: Band, training snr, and sample selection," in *SPAWC*, 2019, pp. 1–5.
- [8] S. Yiet *et al.*, "Interference source identification for ieee 802.15.4 wireless sensor networks using deep learning," in *PIMRC*, 2018, pp. 1–7.
- [9] S. Grunau, D. Block, and U. Meier, "Multi-label wireless interference classification with convolutional neural networks," in *INDIN*, 2018, pp. 187–192.
- [10] M. Schmidt, D. Block, and U. Meier, "Wireless interference identification with convolutional neural networks," in *INDIN*, 2017, pp. 180–185.
- [11] G. Wanget *et al.*, "Classification methods with signal approximation for unknown interference," *IEEE Access*, vol. 8, pp. 37933–37945, 2020.
- [12] Z. Yang, Y. Wang, L. Zhang, and Y. Shen, "Indoor interference classification based on wifi channel state information," in *SpaCCS*, 2018, pp. 136–145.
- [13] C.-J. Liu, P. Huang, L. Xiao, and A.-H. Esfahanian, "Inter-femtocell interference identification and resource management," *IEEE Trans. Mob. Comput.*, vol. 19, no. 1, pp. 116–129, 2020.
- [14] Y. Guo *et al.*, "Regression-based uplink interference identification and sinr prediction for 5g ultra-dense network," in *ICC*, 2020, pp. 1–6.
- [15] S. Grimaldi, A. Mahmood, and M. Gidlund, "An SVM-Based Method for Classification of External Interference in Industrial Wireless Sensor and Actuator Networks," *J. Sens. Actuar. Netw.*, vol. 6, no. 2, pp. 9, 2017.
- [16] T. Mo, Z. Hao, and Y. Tang, "Iterative DS-CDMA Anti-interference Technique Based on Interference Power Cognition," in *WICON*, 2011, pp. 117–124.
- [17] X. Liu, K. C. Teh, and E. Gunawan, "Interference Identification and Blind Multisensor Detection for Asynchronous CDMA Systems With Multipath Fading," *IEEE Trans. Commun.*, vol. 55, no. 12, pp. 2257–2260, 2007.
- [18] L. Li, "Research and Implementation of Interference Recognition," Xidian University, 2014 (in Chinese).
- [19] G. Wanget *et al.*, "Classification methods with signal approximation for unknown interference," *IEEE Access*, vol. 8, pp. 37933–37945, 2020.
- [20] X. Liu, "Research on Scenario Recognition Based on Deep Learning in Wireless Communication," Xidian University, 2018 (in Chinese).
- [21] I. Goodfellow, Y. Bengio, and A. Courville, "Deep Learning," MIT Press, 2016.
- [22] Cohen and Leon, "Generalized phase-space distribution functions," *J. Math. Phys.*, vol. 7, no. 5, pp. 781–786, 1966.
- [23] W. Heisenberg, "The actual content of quantum theoretical kinematics and mechanics," *Zhurnal Physik*, vol. 43, no. 3-4, pp. 172–198, 1983.
- [24] Y. Luan, Y. Huang, X. Zheng, and J. Cheng, "Seismic time-frequency analysis based on entropy-optimized paul wavelet transform," *IEEE Geosci. Remote S.*, vol. 17, no. 2, pp. 342–346, 2020.
- [25] M. Hatami, M. Farrokhifard, and M. Parniani, "A non-stationary analysis of low-frequency electromechanical oscillations based on a refined margenau-hill distribution," *IEEE Trans. Power Syst.*, vol. 31, no. 2, pp. 1567–1578, 2016.
- [26] M. Zhang, M. Diao, and L. Guo, "Convolutional neural networks for automatic cognitive radio waveform recognition," *IEEE Access*, vol. 5, pp. 11074–11082, 2017.
- [27] R. C. Gonzalez and R. E. Woods, "Digital image processing," *Prentice Hall International*, vol. 28, no. 4, pp. 484–486, 2008.
- [28] J. Bromley, I. Guyon, Y. Lecun, E. Sckinger, and R. Shah, "Signature verification using a siamese time delay neural network," in *NIPS*, 1993.

- [29] G. Koch, R. Zemel, R. Salakhutdinov *et al.*, “Siamese neural networks for one-shot image recognition,” in *ICML*, pp. 1–8, 2015.
- [30] A. Krizhevsky, I. Sutskever, and G. Hinton, “Imagenet classification with deep convolutional neural networks,” *Commun. ACM*, vol. 60, no. 6, pp. 84–90, 2017.